

RESEARCH

Open Access



Dysregulated gastric microbial communities and functional shifts in chronic atrophic versus non-atrophic gastritis: a *Helicobacter pylori*-Negative observational study

Hong Yao^{1,2,3}, Tingting Liu^{2,3}, Yiming Chen^{2,3}, Ling She^{2,3}, Tingfeng Wu^{2,3}, Dongsong Liu^{2,3}, Yuhong Deng^{2,3}, Yubin Han^{2,3}, Kai Chen^{2,3}, Jianmin Deng^{2,3}, Jue Zhang^{2,3}, Jinfeng Chen^{2,3*} and Fengbin Liu^{4,5*}

Abstract

Background *Helicobacter pylori* (*H. pylori*) infection was identified as a substantial risk factor for gastric cancer development, but the eradication of *H. pylori* did not necessarily lead to a reduction in the incidence of gastric cancer. Non-*Helicobacter pylori* (*non-H. pylori*) bacteria in the stomach are involved in the transformation of gastritis carcinoma. The aim of this study was to characterize the microbiome composition of the gastric mucosa and its functions in *non-H. pylori* (*H. pylori*-negative) patients with chronic atrophic gastritis (CAG) and chronic non-atrophic gastritis (CNAG).

Methods Fourteen CNAG samples and twenty-three CAG samples were collected. The composition of the gastric microbiome was analyzed using 16 S rDNA gene sequencing. The bioinformatic analysis was performed using alpha and beta diversity analyses, PICRUSt2, and linear discriminant analysis effect size (LEfSe).

Results The two groups shared the same most abundant bacterial phyla (Pseudomonadota, Bacillota, Actinomycetota, and Bacteroidota). The top 5 most abundant bacterial genera in the CAG group were *Sphingomonas*, *Ralstonia*, *Brevundimonas*, *Methyloversatilis*, and *Pseudomonas*. In the CNAG group, the top genera were *Brevundimonas*, *Ralstonia*, *Sphingomonas*, *Methyloversatilis*, and *Acinetobacter*. Differential analysis revealed distinct genera between groups: the CAG group showed enrichment in *Sphingomonas*, *Ralstonia*, *Bradyrhizobium*, *Roseateles*, and *Acidithiobacillus*, while the CNAG group was enriched in *Brevundimonas*, *Rhodococcus*, *Hydrogenophaga*, *Bacteroides*, and *Leifsonia* ($p < 0.05$). *Sphingomonas* exhibited a positive correlation with *Acidithiobacillus* but negative correlations with *Brevundimonas*, *Hydrogenophaga*, and *Leifsonia*. Pathways related to xenobiotic biodegradation, metabolism, signal transduction, cofactor/vitamin metabolism, cancer, infectious diseases, and digestive system were enriched in the CAG group. In contrast, the CNAG group showed enrichment in amino acid metabolism, translation, replication/repair, and terpenoid/polyketide metabolism.

*Correspondence:
Jinfeng Chen
fscjf@sina.com
Fengbin Liu
liufengbin163@163.com

Full list of author information is available at the end of the article



© The Author(s) 2025. **Open Access** This article is licensed under a Creative Commons Attribution-NonCommercial-NoDerivatives 4.0 International License, which permits any non-commercial use, sharing, distribution and reproduction in any medium or format, as long as you give appropriate credit to the original author(s) and the source, provide a link to the Creative Commons licence, and indicate if you modified the licensed material. You do not have permission under this licence to share adapted material derived from this article or parts of it. The images or other third party material in this article are included in the article's Creative Commons licence, unless indicated otherwise in a credit line to the material. If material is not included in the article's Creative Commons licence and your intended use is not permitted by statutory regulation or exceeds the permitted use, you will need to obtain permission directly from the copyright holder. To view a copy of this licence, visit <http://creativecommons.org/licenses/by-nc-nd/4.0/>.

Conclusion Gastric mucosal microbiota dysbiosis and functional shifts are significantly associated with chronic atrophic gastritis. Taxa such as *Sphingomonas* and *Ralstonia*, enriched in CAG patients, may indicate microbial signatures associated with early atrophic transition and provide candidates for further mechanistic validation.

Keywords Chronic atrophic gastritis, *Helicobacter pylori*-negative gastritis, Gastric microbiota dysbiosis, 16S rDNA sequencing, Metabolic prediction

Introduction

The term chronic gastritis refers to inflammatory lesions of the gastric mucosa caused by various etiologies, primarily classified based on the presence or absence of gastric mucosal atrophy into chronic non-atrophic gastritis or chronic atrophic gastritis [1, 2]. The Correa cascade, describing the progression of gastric adenocarcinoma (CNAG → CAG → intestinal metaplasia → dysplasia → gastric cancer), is widely accepted [3]. As CAG with intestinal metaplasia represents a precancerous state, current research prioritizes intercepting this progression [4, 5]. While *Helicobacter pylori* (*H. pylori*) infection poses a substantial risk for developing gastric cancer; nevertheless, the occurrence rate remains below 3% in infected individuals, and eradicating *H. pylori* does not hinder the progression of gastric cancer [6, 7]. Studies have demonstrated the significant contribution of non-*H. pylori* bacteria in the stomach to the maintenance of the gastric environment and overall human health [8]. The prevailing consensus is that the gastric microbiota exerts a significant influence on the process of carcinogenesis [9]. The presence of chronic atrophic gastritis plays a pivotal role in the progression toward intestinal-type gastric cancer [3], and the presence of non-*H. pylori* microbiota in the gastric environment might significantly contribute to the pathogenesis of chronic gastritis.

16 S rDNA sequencing enables high-throughput sequencing of bacterial communities in specific environmental or host-derived samples, facilitating the study of microbial community composition, interpretation of diversity, richness, and population structure, and exploration of the relationships between microorganisms and their environment or host. Currently, it has been extensively employed in research to analyze the structural organization and abundance of gastric microorganisms [10, 11].

In our study, gastric biopsies were collected from patients who required upper endoscopy, and the patients were categorized into two groups based on the results of histologic examination and breath tests. Utilizing 16 S rDNA sequencing to investigate the gastric microbiome composition in patients with CNAG and CAG may enhance our understanding of the pathogenesis of gastritis, and offer novel insights and approaches for disease diagnosis and treatment.

Materials and methods

Patients

This cross-sectional study included patients with chronic gastritis who underwent upper gastrointestinal endoscopy at Foshan Hospital of Traditional Chinese Medicine between August 2022 and August 2023. The diagnostic criteria were established according to the 2022 edition of the Chinese Guidelines for Chronic Gastritis [12], and the diagnosis was confirmed based on the results of gastroscopy and histopathological examination. The inclusion criteria were: (a) patients who were older than 18 years and younger than 80 years; (b) patients who did not take antibiotics, proton-pump inhibitors, H2 receptor antagonists, bismuth agents, or mucosal protective agents within the 4 weeks prior to enrollment; (c) patients who did not undergo gastrectomy; and (d) patients without gastric cancer (GC) or other malignancies. The exclusion criteria were as follows: (a) patients who refused to receive upper gastrointestinal endoscopy; (b) patients who were not suitable for upper gastrointestinal endoscopy, including those with high blood pressure, abdominal pain, and/or asthma; and (c) patients with a positive 13–14 C breath test results. Consecutive patients meeting the eligibility criteria were enrolled during the study period. Patients were consecutively enrolled without stratification to reflect real-world clinical practice. The sample size was determined based on the availability of eligible patients during the study period, consistent with similar microbiome studies [13].

A total of 37 participants were included in this research. The individuals were divided into two groups based on the histological characteristics of their gastric mucosa and their *H. pylori* infection status.

Sample collection

Two pieces of gastric antrum mucosal tissue were obtained at the same location by endoscopic biopsy from each enrolled patient. One sample was processed for histological examination, and the other sample was stored in sterile cryovials at – 80 °C for bacterial DNA extraction.

Bacterial DNA extraction

As directed by the manufacturer, CTAB was used to extract the DNA from the samples. It has been demonstrated that this reagent, which is used to extract DNA from minute amounts of material, works well for most bacteria. Nuclease-free water served as the blank. After

the whole DNA was eluted in 50 μ L of elution buffer, it was kept at -80°C until LC-Bio Technology Co., Ltd (Hangzhou, China), was detected via PCR.

PCR amplification and 16 S rDNA sequencing

After amplifying the variable 16S rDNA V3-V4 regions [14], a fragment gene library was created. The forward primer 341F (5'-CCTACGGGNGGCWGCAG-3') and the reverse primer 805R (5'-GACTACHVGGGTATCTAATCC-3') were utilized. For each sample and the sequencing universal primers, unique barcodes were applied to the 5' ends of the primers. A total of 25 μ L of reaction mixture which included 2.5 μ L of each primer, 12.5 μ L of PCR Premix, and PCR-grade water to regulate the volume was used for PCR amplification. Prokaryotic 16 S fragments were amplified using PCR under the following conditions: 30 s of initial denaturation at 98°C , 32 cycles of denaturation at 98°C for 10 s, annealing at 54°C for 30 s, and extension at 72°C for 45 s, with a final extension at 72°C for 10 min. Electrophoresis on a 2% agarose gel was used to validate the PCR results. Throughout the DNA extraction procedure, ultrapure water was utilized as a negative control in place of a sample solution to reduce the risk of false-positive PCR results. Qubit[®] (Invitrogen, USA) was used to quantify the PCR products after they had been purified using AMPure XT beads (Beckman Coulter Genomics, Danvers, MA, USA). The amplified pools were prepared for sequencing, and the size and quantity of the amplicon library were evaluated using an Agilent 2100 Bioanalyzer (Agilent, USA) and an Illumina Library Quantification Kit (Kapa Biosciences, Woburn, MA, USA), respectively. Libraries were sequenced on an Illumina NovaSeq PE250 platform.

Bioinformatic processing

The samples were sequenced on an Illumina NovaSeq platform following the manufacturer's recommendations provided by LC-Bio. Paired-end reads were assigned based on the unique barcode of each sample and then truncated by removing the barcode and primer sequence. Subsequently, FLASH was used to merge paired-end reads. The raw reads were subjected to quality filtering using fqtrim v0.94 under specific conditions to eliminate low-quality sequences and obtain high-quality clean tags. Vsearch software (v2.3.4) was used for further screening of chimeric sequences, while DADA2 [15] performed dereplication to generate feature lists and sequences. The sequence numbers were randomly normalized to ensure consistency across all samples. Samples with missing sequencing data or failed PCR amplification were excluded from the analysis. Bioinformatic processing (QIIME2 [16]) included amplicon sequence variant (ASV) generation and diversity calculations, followed by taxonomic annotation of ASVs via SILVA database alignment

(BLAST). Subsequently, feature abundance was normalized based on the relative abundance of each sample.

Statistical analysis

For continuous variables, data normality was assessed using the Shapiro–Wilk test. Normally distributed variables are presented as mean \pm standard deviation (SD) and analyzed via the independent samples t-test. Non-normally distributed variables are summarized as median (interquartile range, IQR) and compared using the Mann-Whitney U test. Categorical variables were expressed as frequencies and percentages. Group comparisons were performed using the chi-square test, with a two-tailed p -value < 0.05 considered statistically significant. Bacterial abundance and diversity were assessed using alpha diversity analysis, with results described by the Shannon index, Chao1 index, and Observed Species. The similarity of bacterial composition was evaluated through beta diversity analysis. Principal component analysis (PCA), nonmetric multidimensional scaling analysis, and ANOSIM were employed to demonstrate differences among the samples. The statistical analysis was performed using IBM SPSS Statistics v29.0 and R v4.1.0. The biomarkers were categorized into two groups using linear discriminant analysis (LDA) effect size (LEfSe). The correlation analysis of bacterial genera was performed using a Spearman network and corrplot, with a threshold for the correlation coefficient $|\rho| > 0.4$. Functional pathway predictions were performed using PICRUST2 (Phylogenetic Investigation of Communities by Reconstruction of Unobserved States) with the KEGG database. Differential abundance of functional pathways was statistically assessed using STAMP v2.1.3 (Statistical Analysis of Metagenomic Profiles) with two-tailed Welch's t-test ($p < 0.05$). Nonparametric ANCOVA (Quade's test) was applied to adjust for age effects on alpha diversity and ASV abundance after rank transformation of age. For beta diversity, PERMANOVA with rank-transformed age as a covariate was implemented using 999 permutations (vegan package in R).

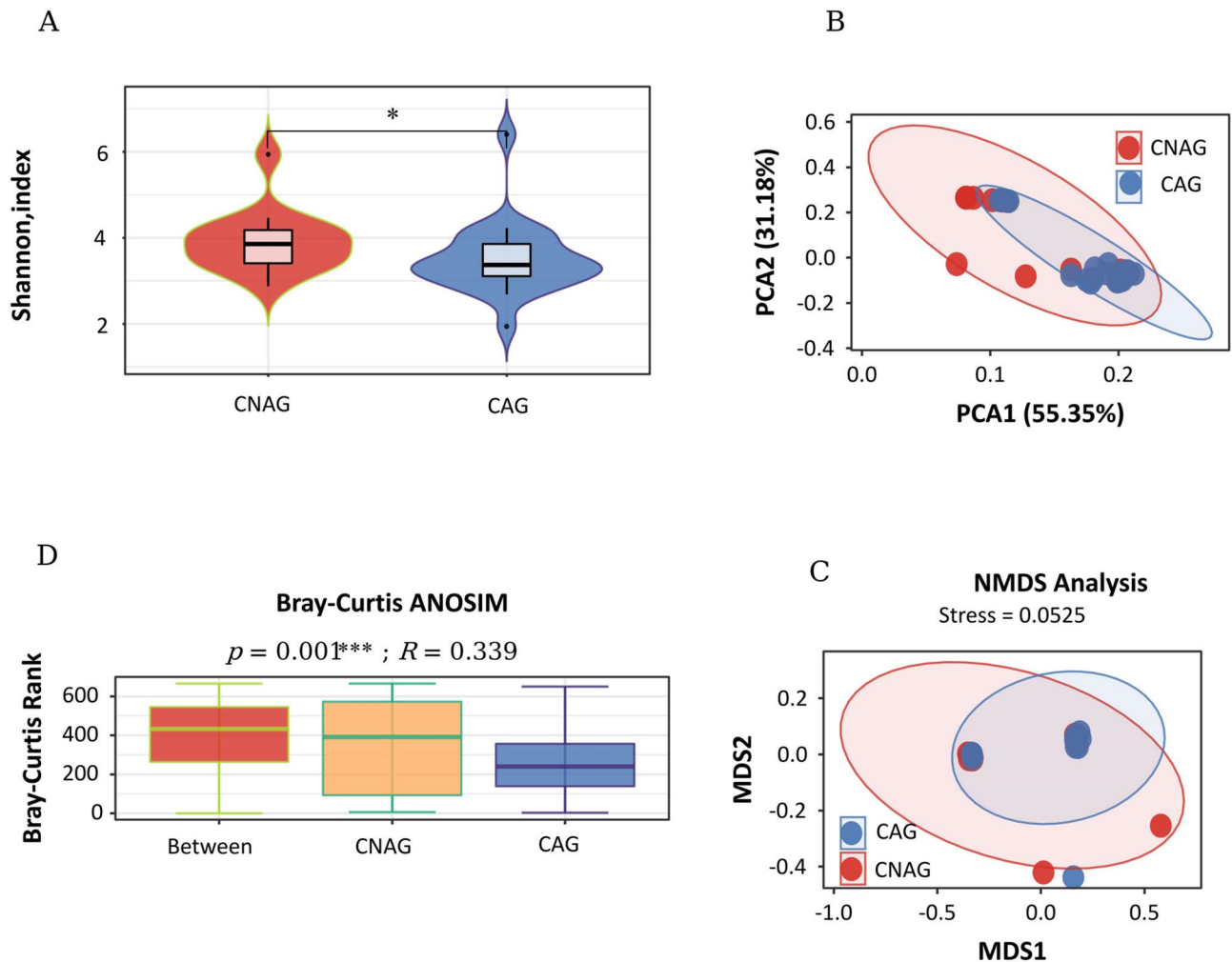
RESULTS

Patient characteristics

During the study period, based on diagnostic and inclusion criteria, 27 patients were initially enrolled in the chronic atrophic gastritis (CAG) group. Among them, 3 patients were excluded due to insufficient gastric mucosal tissue for DNA extraction, and 1 patient was excluded owing to highly divergent sequencing data. Similarly, 27 patients were initially enrolled in the chronic non-atrophic gastritis (CNAG) group, with 12 patients excluded due to inadequate DNA extraction from gastric mucosal samples and 1 patient excluded because of anomalous sequencing data. Consequently, a total of 37 patients

Table 1 Clinical characteristics of patients who underwent CNAG or CAG ($n=37$), ***, $p \leq 0.001$

Group	Age (years), median (IQR)	Z value	p value	Sex/male, (n/%)	χ^2	p value
CAG	57(50–61)	-17.475	<0.001***	8 (34.78)	0.836	0.493
CNAG	48(39–54)			7 (50)		

**Fig. 1** Analysis of alpha and beta diversity. **(A)** Shannon index determined through a violin plot with the Wilcoxon signed-rank test ($p=0.049$). **(B)** Principal component analysis of ASV abundance. **(C)** Non-metric multidimensional scaling of the Bray-Curtis distance. **(D)** ANOSIM analysis indicated a statistically significant difference (ANOSIM $R=0.339$, $p=0.001$). *: $p \leq 0.05$, **: $p \leq 0.01$, ***: $p \leq 0.001$

were ultimately included in the analysis: 23 in the CAG group and 14 in the CNAG group. All patients with chronic atrophic gastritis were pathologically confirmed to exhibit intestinal metaplasia. Complete clinical data were available for all 37 participants; no missing values were observed for age, sex, or histologic diagnosis. The characteristics of the patients are shown in Table 1. Both chronic non-atrophic gastritis (CNAG) and chronic atrophic gastritis (CAG) groups exhibited non-normal age distributions (Shapiro-Wilk test: CNAG, $W=0.935$, $p < 0.001$; CAG, $W=0.910$, $p < 0.001$), necessitating the use of non-parametric statistical analyses. There were no significant sex-related differences between the two groups, but there were significant age-related differences.

This suggested a correlation between the progression of chronic gastritis and age.

Microbiome abundance and diversity

Microbial community abundance and diversity were assessed using the Shannon index, Chao1 index, and Observed Species. While the Shannon index differed significantly between CAG and CNAG groups ($p=0.049$) (Fig. 1A), no statistical significance was observed for the Chao1 index ($p=0.057$) or Observed Species ($p=0.062$), likely due to the limited sample size reducing statistical power to detect richness differences. Principal component analysis (PCA) and non-metric multidimensional scaling (NMDS) of Bray-Curtis distances were used to

compare bacterial community structures between groups (Fig. 1B, C). Analysis of Similarity (ANOSIM) further confirmed significant differences in microbial composition ($R = 0.339$, $p = 0.001$) (Fig. 1D).

Despite the significant age difference between CAG and CNAG groups ($p < 0.001$, Table 1), age-adjusted analyses revealed no confounding effects of age on alpha diversity (Chao1: $p = 0.128$; Observed Species: $p = 0.135$; Shannon: $p = 0.149$) or ASV-level microbial abundance ($p = 0.126$). In contrast, age explained 17.19% of beta diversity variation ($p = 0.004$, PERMANOVA), though the primary group distinction (CAG vs. CNAG) remained robust after adjustment ($p = 0.001$). This suggests that microbiome structural divergence between groups is driven by pathological progression rather than age-related factors.

Bacterial compositions

At the phylum level, the two groups had the same most abundant bacterial phyla (Pseudomonadota, Bacillota, Actinomycetota, and Bacteroidota), although there was a difference in richness between the two groups (Fig. 2A). At the genus level, the top 5 most abundant bacterial

genera in the CAG group were *Sphingomonas*, *Ralstonia*, *Brevundimonas*, *Methyloversatilis*, and *Pseudomonas*, while in the CNAG group, they were *Brevundimonas*, *Ralstonia*, *Sphingomonas*, *Methyloversatilis*, and *Acinetobacter* (Fig. 2B). The two groups had 27 common bacterial phyla and 476 common bacterial genera (Fig. 2C, D).

Comparative analysis of significant microbial differences between two groups

LefSe analysis identified distinct microbial biomarkers between the CAG and CNAG groups through a two-step statistical approach. First, taxa with significant abundance variations (Wilcoxon rank-sum test, $\alpha = 0.05$) were filtered, followed by linear discriminant analysis (LDA) to quantify group-specific effect sizes. Taxonomic hierarchies of these discriminative biomarkers were visualized in a cladogram (Fig. 3A), where yellow and green nodes represent lineages enriched in the CAG and CNAG groups, respectively. Node sizes reflect the log₁₀-transformed LDA scores, emphasizing taxa with stronger associations (LDA > 3.0, Kruskal-Wallis test $p < 0.05$). The cladogram highlights divergent evolutionary branches

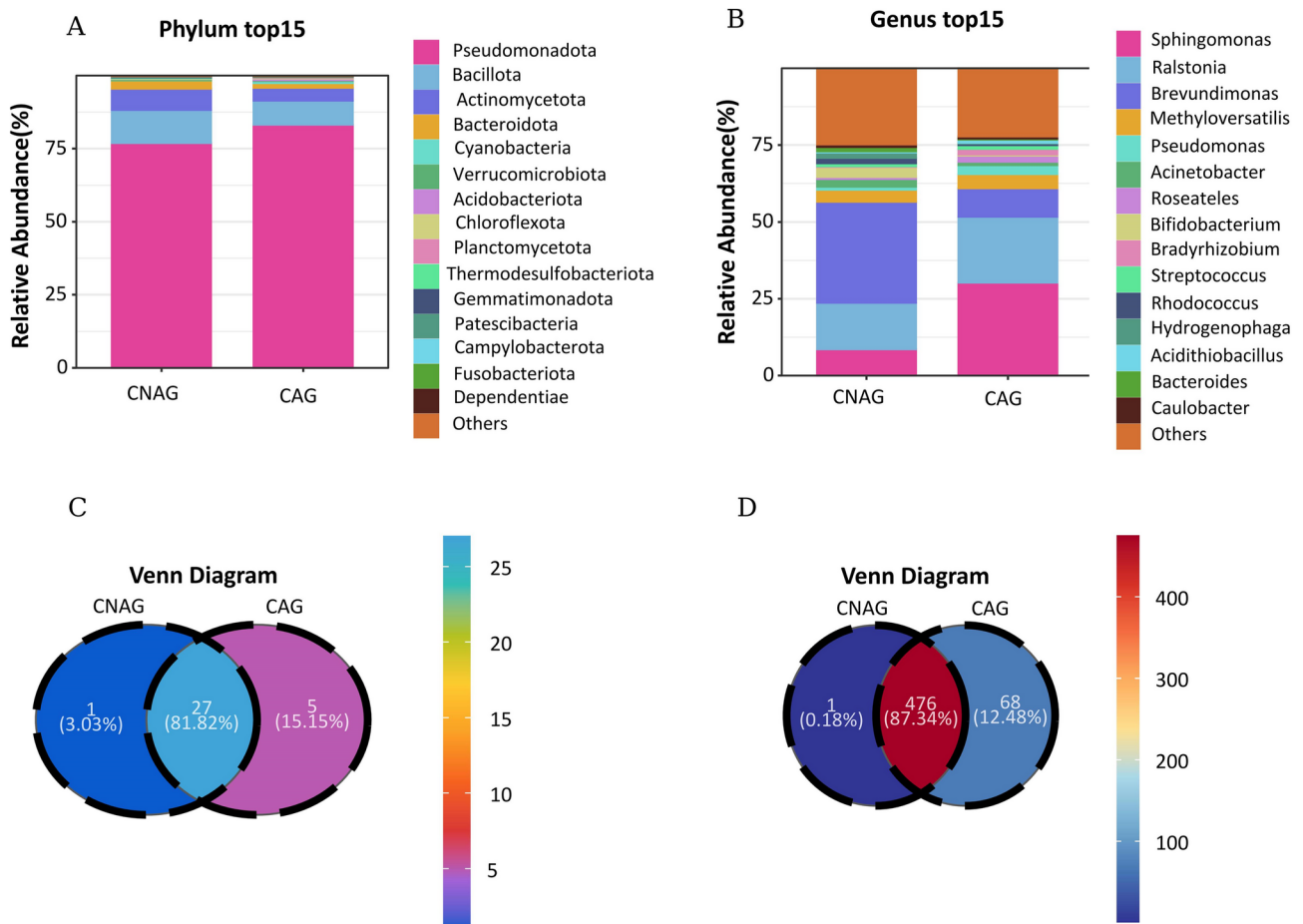


Fig. 2 Bacterial compositions of CAG and CNAG. **(A)** Bacterial phylum-level composition. **(B)** Bacterial genus-level compositions. **(C)** Venn diagram of the proportion of bacterial phyla. **(D)** Venn diagram of the distribution of bacterial genera

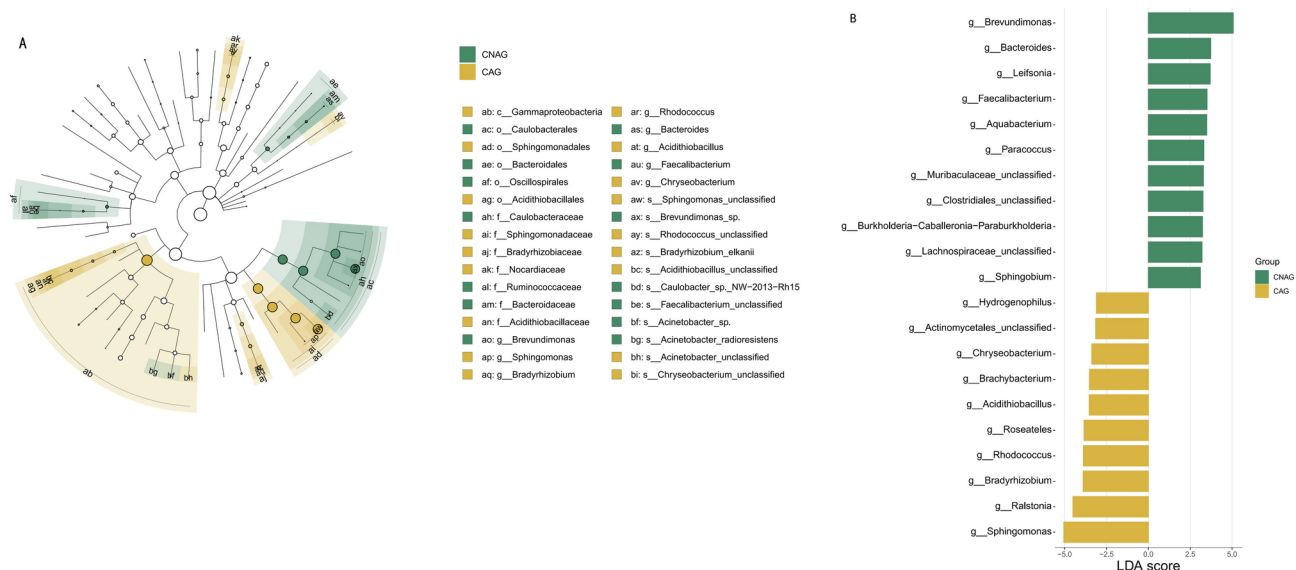


Fig. 3 (A) The cladogram illustrates taxonomic hierarchies of microbial biomarkers significantly associated with the CAG (yellow nodes) and CNAG (green nodes) groups. Node size corresponds to the LDA effect size (log10-transformed), with larger nodes indicating stronger group-specific associations. Colored branches highlight taxonomic lineages enriched in each group (yellow: CAG; green: CNAG). Only taxa meeting a significance threshold of $p < 0.05$ (Kruskal-Wallis test) and LDA score > 3.0 are displayed. (B) Horizontal bars represent the LDA scores (log10-transformed) of bacterial genera significantly enriched in the CAG (yellow) or CNAG (green) groups. Statistical thresholds: $p < 0.05$

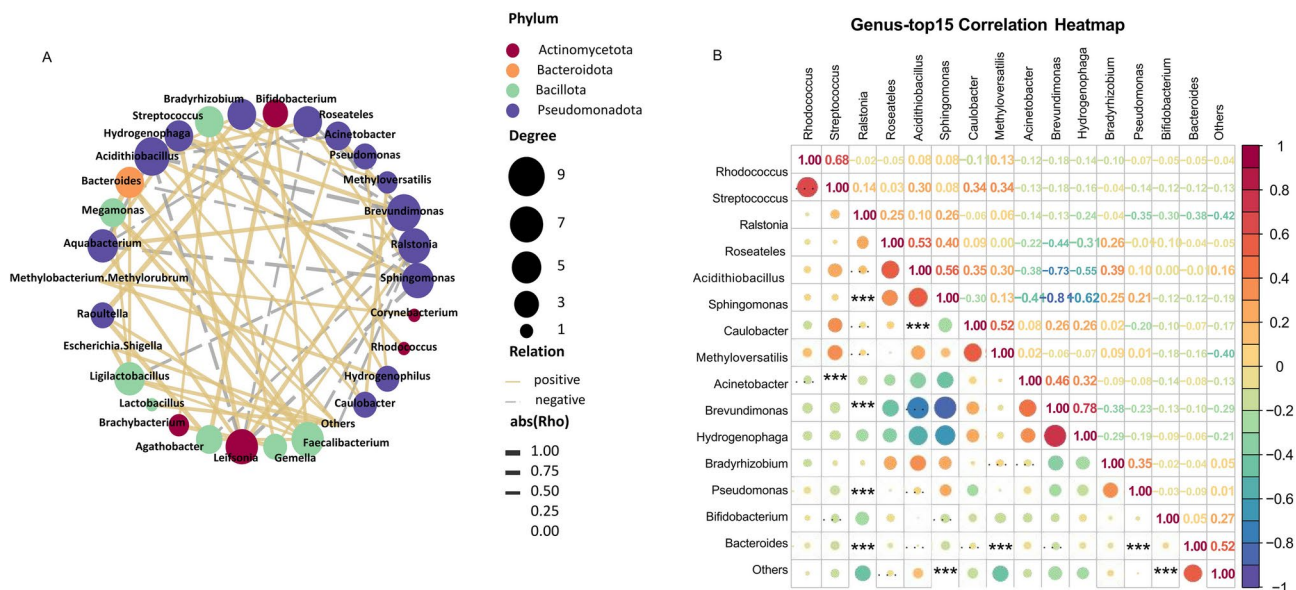


Fig. 4 (A) Correlation network of the top 30 differentially abundant bacterial genera. Nodes: Color indicates bacterial phylum; size reflects degree centrality (number of connections). Edges: Significant correlations (Spearman's $\rho > 0.4$, $p < 0.05$, FDR-adjusted); thickness indicates strength; solid lines = positive ($\rho > 0.4$), dashed lines = negative ($\rho < -0.4$). (B) Pairwise Spearman correlations between genera. Color intensity and hue denote correlation strength and direction (red: positive, blue: negative; $|\rho| > 0.4$, $p < 0.05$). Coefficients are annotated numerically. Lower left: Statistical significance of correlations (p -values). Significance levels: * $p \leq 0.05$, ** $p \leq 0.01$, *** $p \leq 0.001$.

dominated by CAG-associated taxa (e.g., *Sphingomonas*, *Ralstonia*, *Roseateles*) and CNAG-enriched genera (e.g., *Brevundimonas*, *Bacteroides*). At the genus level (Fig. 3B), 10 taxa showed significant enrichment in the CAG group (LDA scores > 3.0 , yellow bars), while 11 genera were overrepresented in the CNAG group (green bars).

Inter-Species correlation analysis of bacterial taxa

Microbial co-occurrence patterns were analyzed through correlation heatmaps and network analysis ($|\rho| > 0.4$ threshold) (Fig. 4A, B). Key interactions included: *Sphingomonas* exhibited positive correlations with *Acidithiobacillus* and *Roseateles*, while showing negative

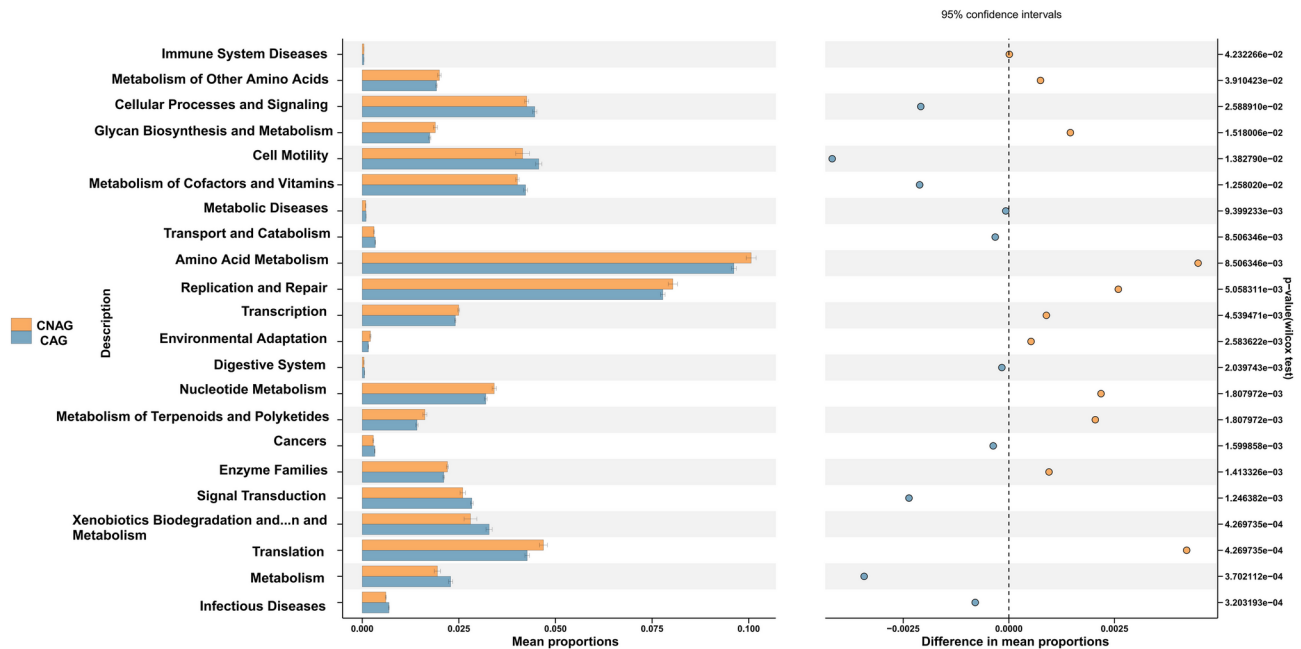


Fig. 5 Functional pathway prediction analysis of gastric microbiota (KEGG Level 2). Left panel: Relative abundance of KEGG pathways with significant differences ($p < 0.05$, Wilcoxon rank-sum test) between CNAG (yellow bars) and CAG (blue bars). The y-axis lists pathway categories; the x-axis represents the relative proportion of each pathway in the two groups. Right panel: Effect size and 95% confidence intervals of differentially abundant pathways. The x-axis shows the difference in pathway proportions (CAG vs. CNAG); the y-axis displays the corresponding p -values. Dots represent individual pathways; horizontal lines indicate 95% confidence intervals

associations with *Brevundimonas*, *Hydrogenophaga*, and *Leifsonia*. *Brevundimonas* demonstrated contrasting relationships: Positive correlations with *Hydrogenophaga*, *Leifsonia*, *Aquabacterium*, and *Acinetobacter*; Negative correlations with *Sphingomonas* and *Acidithiobacillus*.

Functional features of the gastric microbiota

As shown in Fig. 5, PICRUSt2 suggested potential functional alterations. Pathways related to xenobiotic biodegradation, metabolism, cofactor/vitamin metabolism, cancer, infectious diseases, and digestive system-related pathways were enriched in the CAG group. In contrast, the CNAG group showed enrichment in amino acid metabolism, translation, replication/repair, and terpenoid/polyketide metabolism (Fig. 5).

Discussion

Based on the Corrêa cascade, *H. pylori* infection was identified as a substantial risk factor for gastric cancer development. Nevertheless, after undergoing *H. pylori* eradication treatment, the risk of gastric cancer decreased by less than 50% [17]. As demonstrated in the current study, solely employing *H. pylori* eradication therapy did not prove to be an effective method for preventing the progression of gastric precancerous lesions [18, 19]. Studies demonstrate that in the Insulin-Gastrin (INS-GAS) transgenic mouse model, mice carrying gastric-specific pathogen-free microbiota developed more

severe gastric precancerous lesions compared to *H. pylori* mono-infected controls [20]. Furthermore, transplantation of gastric microbiota and fluids from human patients with intestinal metaplasia or gastric cancer successfully induced precancerous features in germ-free mice, whereas *H. pylori* mono-infection alone failed to replicate this carcinogenic progression [21–23]. Collectively, these findings suggest that non-*H. pylori* gastric microbiota may participate in the pathological progression from chronic gastritis to gastric cancer. Given that chronic atrophic gastritis (CAG) and intestinal metaplasia (IM) are obligatory precursors of intestinal-type gastric cancer, elucidating microbial taxa and functional pathways associated with these precancerous states is critical.

In our study, we confirmed the microbiome composition in the gastric mucosal tissues of individuals with chronic non-atrophic gastritis and chronic atrophic gastritis. Our findings revealed a notable decrease in microbial diversity among patients with intestinal metaplasia and chronic atrophic gastritis compared to those with chronic non-atrophic gastritis [24, 25]. Similarly, the abundance of gastric microorganisms from CAG-PLGC-GC (Chronic Atrophic Gastritis-Precancerous Lesions-Gastric Cancer) gradually decreased. Similarly, other studies also indicated that compared with that in non-atrophic gastritis, the microbial richness of intestinal metaplasia and gastric cancer patients was significantly reduced [25–28].

At the taxonomic level, Pseudomonadota, Bacillota, Actinomycetota, and Bacteroidota were the four predominant phyla shared by both groups, consistent with previous studies [28]. The abundance of Pseudomonadota increased from chronic non-atrophic gastritis to chronic atrophic gastritis, while the relative abundance of Bacillota, Actinomycetota, and Bacteroidota decreased during this transition. This was in line with previous research findings [29].

At the genus level, in the atrophic gastritis group, the five bacterial genera with the greatest abundance were identified as *Sphingomonas*, *Ralstonia*, *Brevundimonas*, *Methyloversatilis*, and *Pseudomonas*. Conversely, in the non-atrophic gastritis group, *Brevundimonas*, *Ralstonia*, *Sphingomonas*, *Methyloversatilis*, and *Acinetobacter* were found to be the top five bacterial genera. The prevalence of *Sphingomonas*, *Ralstonia*, *Bradyrhizobium*, *Roseateles* and *Acidithiobacillus* increased from chronic non-atrophic gastritis to chronic atrophic gastritis; conversely, the relative prevalence of *Brevundimonas*, *Rhodococcus*, *Hydrogenophaga*, *Bacteroides* and *Leifsonia* decreased during this transition. There were discernible disparities among these bacterial genera. One study [30] also revealed an enrichment of *Sphingomonas*, *Ralstonia*, and *Roseateles* in bladder cancer tissue. Furthermore, these bacteria might play a role in the degradation of polycyclic aromatic hydrocarbons, which are a class of organic pollutants that exert detrimental effects on both human health and the environment [31]. We identified the genus *Acinetobacter* (phylum Pseudomonadota), a group of Gram-negative opportunistic pathogens frequently implicated in nosocomial infections. Notably, recent studies have reported elevated abundance of *Acinetobacter* in mucosal dysplastic lesions compared to adjacent healthy tissues [13, 32]. Furthermore, studies have indicated that *Acinetobacter lwoffii* and *Streptococcus anginosus* were associated with persistent gastric inflammation [32–34].

We identified significant correlations and associations using Spearman network analysis of the gastric microbiota. *Sphingomonas* exhibited positive correlations with *Acidithiobacillus* and *Roseateles*, while showing negative associations with *Brevundimonas*, *Hydrogenophaga*, and *Leifsonia*. Functional pathway predictions via PICRUSt2 suggested potential alterations in the metabolic potential of gastric microbial communities in chronic atrophic gastritis. These included a relative enrichment in pathways linked to cofactor and vitamin metabolism and xenobiotic biodegradation, alongside a relative decrease in amino acid and nucleotide metabolism (see Fig. 5). Notably, these predictions reflect inferred functional capacities based on 16 S rRNA gene data and require further validation through direct metabolic profiling or multi-omics approaches. Changes in gastric microorganisms during the progression from chronic nonatrophic

gastritis to chronic atrophic gastritis might weaken the synthesis of amino acids and nucleotides, as well as the regulation and expression of proteins. Signal transduction might also be adjusted to increase the demand for exogenous biodegradation and cofactors and vitamins. This indicated that the microorganisms in the stomach might play a role in promoting chronic inflammation through these mechanisms. Alterations in the gastric microbiota might lead to the depletion of parietal cells and an increase in inflammatory *foci* [21].

Some limitations of our study should be considered. First, The modest cohort size ($n=37$) likely constrained our ability to detect subtle intergroup differences in bacterial genus abundances between chronic atrophic gastritis (CAG) and chronic non-atrophic gastritis (CNAG) patients. This limitation is further supported by the non-significant trends observed in alpha diversity metrics quantifying species richness, including the Chao1 index ($p=0.128$) and Observed Species ($p=0.135$), despite significant differences in Shannon diversity ($p=0.049$). To definitively characterize microbial richness variations during atrophic transition, validation through large-scale multicenter studies is imperative. However, 24 bacterial genera were identified in our study, although some bacterial genera have been reported in other studies. While age contributed to beta diversity variation, its confounding effect on alpha diversity and differentially abundant ASVs was negligible. This underscores that the observed microbiome differences between CAG and CNAG groups are independent of age. Nevertheless, future studies should explore age-microbiome interactions in larger cohorts to validate these findings. Second, we did not evaluate the changes of significantly different bacterial genera during the progression from chronic nonatrophic gastritis to chronic atrophic gastritis, intestinal metaplasia, dysplasia or gastric cancer, which might further provide valuable insights into the identification of different bacterial genera at different pathological stages of gastric cancer transformation. Third, while we did not evaluate novel insights into microbial drivers of gastric inflammation, our findings are derived from a single-center cohort. Future multi-center studies with larger sample sizes are warranted to validate these results, particularly given the multifactorial influences on the human microbiome. And while PICRUSt2 provides a cost-effective approach to hypothesize functional shifts, future studies integrating metagenomic sequencing and metabolomic profiling are essential to validate these predicted metabolic alterations.

In general, the objective of this study was to examine the changes in microbiome composition in patients with CNAG and CAG with a specific focus on *non-H. pylori* individuals. The differentially enriched bacterial genera between CAG and CNAG groups, particularly

Sphingomonas and *Ralstonia*, may indicate microbial signatures associated with early atrophic transition and provide candidates for further mechanistic validation. Additionally, microbes might be involved in biodegradation, metabolism, signal transduction, and inflammation and participate in the modulation of persistent inflammation within neoplastic lesions.

Acknowledgements

This work was supported by the inaugural Postgraduate Training Fund project of Foshan Hospital of Traditional Chinese Medicine in 2023 (No. 20233002).

Author contributions

HY and FBL designed the study and wrote the Manuscript. JZ and TFW analyzed clinical data. TTL, LS, DSL, YMC, YHD, YBH, KC and JMD collected patients and clinical samples. FBL and JFC provided guidance on the study and gave writing-review. All authors read and approved the final version of the manuscript.

Funding

This study was supported by the National Natural Science Foundation of China (Grant No. 82474408), the Science and Technology Program of Foshan City (Grant No. 2220001005125), and the Postgraduate Training Fund of Foshan Hospital of Traditional Chinese Medicine, Affiliated Hospital of Guangzhou University of Chinese Medicine (Grant No. 20233002).

Data availability

All sequencing results were submitted to NCBI with PRJNA1113136 (RUN37597816–RUN37597852).

Declarations

Ethical approval and consent to participate

This study was conducted in accordance with the ethical principles of the Declaration of Helsinki (2013 version). The study protocol obtained prior approval from the Ethics Committee of Foshan Hospital of Traditional Chinese Medicine (Approval No. KY[2022]165). Written informed consent was obtained from all individual participants after they were fully informed about the study purpose, procedures, and potential risks (in accordance with Declaration of Helsinki paragraphs 15, 22–24).

Consent for publication

Not applicable.

Competing interests

The authors declare no competing interests.

Repositories

All sequencing results were submitted to NCBI with PRJNA1113136 (RUN37597816–RUN37597852). This database is now accessible, allowing you to link to the website for inquiries (<https://dataview.ncbi.nlm.nih.gov/object/PRJNA1113136?reviewer=2lj2jcepbs0ltjpp0468b9g88c>).

Author details

¹Guangzhou University of Chinese Medicine, Guangzhou 510405, Guangdong, People's Republic of China

²The Eighth Clinical Medical College of Guangzhou University of Chinese Medicine, Foshan 528000, Guangdong, People's Republic of China

³Foshan Hospital of Traditional Chinese Medicine, Foshan 528000, Guangdong, People's Republic of China

⁴Lingnan Institute of Spleen and Stomach Diseases, The First Affiliated Hospital of Guangzhou University of Chinese Medicine, Guangzhou 510405, Guangdong, People's Republic of China

⁵Baiyun Hospital of the First Affiliated Hospital of Guangzhou University of Chinese Medicine, Guangzhou 510080, Guangdong, People's Republic of China

Published online: 29 April 2025

References

- Dixon MF, Genta RM, Yardley JH et al. Classification and grading of gastritis. The updated Sydney System. International Workshop on the Histopathology of Gastritis, Houston 1994.[J]. American Journal of Surgical Pathology. 1996;20(10):1161–1181.<https://doi.org/10.1148/radiology.203.2.434>
- Tytgat GNJ. The Sydney System: endoscopic division. Endoscopic appearances in gastritis/duodenitis. J Gastroenterol Hepatol 6: 223–234[J]. Journal of Gastroenterology & Hepatology, 1991;6(3):223–234.<https://doi.org/10.1111/j.1440-1746.1991.tb01469.x>
- Correa P. Human gastric carcinogenesis: A multistep and multifactorial Process—First American Cancer society award lecture on Cancer epidemiology and Prevention[J]. Cancer research, 1992;52(24):6735–40.
- Hwang YJ, Choi Y, Kim N, et al. The difference of endoscopic and histologic improvements of atrophic gastritis and intestinal metaplasia after Helicobacter pylori eradication. Dig Dis Sci. 2022;67(7):3055–66. <https://doi.org/10.1007/s10620-021-07146-4>. Epub 2021 Aug 7. PMID: 34365533.
- Aumpan N, Vilaichone RK, Pornthisarn B, et al. Predictors for regression and progression of intestinal metaplasia (IM): A large population-based study from low prevalence area of gastric cancer (IM-predictor trial). PLoS ONE. 2021;16(8):e0255601. <https://doi.org/10.1371/journal.pone.0255601>. PMID: 34379655; PMCID: PMC8357097.
- Uemura N, Okamoto S, Yamamoto S et al. Helicobacter pylori infection and the development of gastric cancer. N. Engl. J. Med. 345, 784–789[J]. New England Journal of Medicine. 2001;345(11):784–789.<https://doi.org/10.1056/NEJMoa001999>
- Dias-Jácome E, Libânio, Borges-Canha M, et al. Gastric microbiota and carcinogenesis: the role of non-Helicobacter pylori bacteria: a systematic review[J]. Revista Española De Enfermedades Digestivas. 2016;108. <https://doi.org/10.17235/reed.2016.4261/2016>.
- Ruan W, Engevik MA, Spinler JK, et al. Exploration[J] Dig Dis Sci. 2020;65(3). <https://doi.org/10.1007/s10620-020-06118-4>. Healthy Human Gastrointestinal Microbiome: Composition and Function After a Decade of.
- Scott AJ, Alexander JL, Merrifield CA, et al. International Cancer Microbiome consortium consensus statement on the role of the human Microbiome in carcinogenesis[J]. Gut. 2019;68(9):gutjnl–2019. <https://doi.org/10.1136/gutjnl-2019-318556>.
- Nikitina D, Lehr K, Vilchez-Vargas R, et al. Comparison of genomic and transcriptional Microbiome analysis in gastric cancer patients and healthy individuals. World J Gastroenterol. 2023;29(7):1202–18. <https://doi.org/10.3748/wjg.v29.i7.1202>. PMID: 36926663; PMCID: PMC10011954.
- Yu T, Lu T, Deng W, et al. Microbiome and function alterations in the gastric mucosa of asymptomatic patients with Helicobacter. pylori infection[J]. Helicobacter; 2023.
- Chinese Medical Association, Branch G, Association CM, Branch G, Collaborative Group on Digestive System Tumors, Jingyuan F, et al. Chinese guidelines for the diagnosis and treatment of chronic gastritis (2022, Shanghai) [J]. Gastroenterology. 2023;28(3):149–80. <https://doi.org/10.3969/j.issn.1008-7125.2023.03.004>.
- Logue JB, Stedmon CA, Kellerman AM, et al. Experimental insights into the importance of aquatic bacterial community composition to the degradation of dissolved organic matter. ISME J. 2016;10(3):533–45. <https://doi.org/10.1038/ismej.2015.131>. Epub 2015 Aug 21. PMID: 26296065; PMCID: PMC4817675.
- Callahan BJ, McMurdie PJ, Rosen MJ, et al. DADA2: High-resolution sample inference from illumina amplicon data. Nat Methods. 2016;13(7):581–3. <https://doi.org/10.1038/nmeth.3869>. Epub 2016 May 23. PMID: 27214047; PMCID: PMC4927377.
- Bolyen E, Rideout JR, Dillon MR, et al. Author correction: reproducible, interactive, scalable and extensible Microbiome data science using QIIME 2. Nat Biotechnol. 2019;37(9):1091. <https://doi.org/10.1038/s41587-019-0252-6>. Erratum for: Nat Biotechnol. 2019;37(8):852–857. PMID: 31399723.
- Correa P, Piazzuelo MB, Camargo MC. The future of gastric cancer prevention. Gastric Cancer. 2004;7(1):9–16. <https://doi.org/10.1007/s10120-003-0265-0>. PMID: 15052434.
- Ford AC, Yuan Y, Moayyedi P. Helicobacter pylori eradication therapy to prevent gastric cancer: systematic review and meta-analysis. Gut. 2020;69(12):2113–21. <https://doi.org/10.1136/gutjnl-2020-320839>. Epub 2020 Mar 23. PMID: 32205420.

18. Sung JJ, Lin SR, Ching JY et al. Atrophy and intestinal metaplasia one year after cure of *H. pylori* infection: a prospective, randomized study. *Gastroenterology*. 2000;119(1):7–14. <https://doi.org/10.1053/gast.2000.8550>. PMID: 10889149.
19. Lofgren JL, Whary MT, Ge Z, et al. Lack of commensal flora in *Helicobacter pylori*-infected INS-GAS mice reduces gastritis and delays intraepithelial neoplasia. *Gastroenterology*. 2011;140(1):210–20. <https://doi.org/10.1053/j.gastro.2010.09.048>. Epub 2010 Oct 13. PMID: 20950613; PMCID: PMC3006487.
20. Kwon SK, Park JC, Kim KH, et al. Human gastric microbiota transplantation recapitulates premalignant lesions in germ-free mice. *Gut*. 2022;71(7):1266–76. <https://doi.org/10.1136/gutjnl-2021-324489>. Epub 2021 Aug 13. PMID: 34389621.
21. Shen Z, Dzik-Fox J, Feng Y, et al. Gastric Non-*Helicobacter pylori* Urease-Positive *Staphylococcus epidermidis* and *Streptococcus salivarius* isolated from humans have contrasting effects on *H. pylori*-Associated gastric pathology and host immune responses in a murine model of gastric Cancer. *mSphere*. 2022;7(1):e0077221. <https://doi.org/10.1128/msphere.00772-21>. Epub 2022 Feb 9. PMID: 35138124; PMCID: PMC8826947.
22. Sgamato C, Rocco A, Compare D, et al. Exploring the link between *Helicobacter pylori*, gastric microbiota and gastric Cancer. *Antibiot (Basel)*. 2024;13(6):484. <https://doi.org/10.3390/antibiotics13060484>. PMID: 38927151; PMCID: PMC11201017.
23. Wang Z, Gao X, Zeng R, et al. Changes of the gastric mucosal Microbiome associated with histological stages of gastric Carcinogenesis[J]. *Front Microbiol*. 2020;11. <https://doi.org/10.3389/fmicb.2020.00997>.
24. He C, Peng C, Lu N et al. Convergent dysbiosis of gastric mucosa and fluid microbiome during stomach carcinogenesis. *Gastric Cancer*. 2022;25(5):837–849. <https://doi.org/10.1007/s10120-022-01302-z>. Epub 2022 Jun 4. PMID: 35661945.
25. Liu C, Ng SK, Ding Y, et al. Meta-analysis of mucosal microbiota reveals universal microbial signatures and dysbiosis in gastric carcinogenesis. *Oncogene*. 2022;41(28):3599–610. <https://doi.org/10.1038/s41388-022-02377-9>. Epub 2022 Jun 9. PMID: 35680985; PMCID: PMC9270228.
26. Guo Y, Cao XS, Zhou MG, et al. Gastric microbiota in gastric cancer: different roles of *Helicobacter pylori* and other microbes. *Front Cell Infect Microbiol*. 2023;12:1105811. <https://doi.org/10.3389/fcimb.2022.1105811>. PMID: 36704105; PMCID: PMC9871904.
27. Sun QH, Zhang J, Shi YY, et al. Microbiome changes in the gastric mucosa and gastric juice in different histological stages of *Helicobacter pylori*-negative gastric cancers. *World J Gastroenterol*. 2022;28(3):365–80. <https://doi.org/10.3748/wjg.v28.i3.365>. PMID: 35110955; PMCID: PMC8771614.
28. Lu Y, Liu H, Mao Y, et al. A comprehensive update: Gastrointestinal microflora, gastric cancer and gastric premalignant condition, and intervention by traditional Chinese medicine. *J Zhejiang Univ Sci B*. 2022;23(1):1–18. <https://doi.org/10.1631/jzus.B2100182>. PMID: 35029085; PMCID: PMC8758937.
29. Bukavina L, Isali I, Ginwala R, et al. Global Meta-analysis of urine microbiome: colonization of polycyclic aromatic Hydrocarbon-degrading Bacteria among bladder Cancer patients. *Eur Urol Oncol*. 2023;6(2):190–203. <https://doi.org/10.1016/j.euo.2023.02.004>. Epub 2023 Mar 1. PMID: 36868921.
30. Premnath N, Mohanrasu K, Guru Raj Rao R, et al. A crucial review on polycyclic aromatic Hydrocarbons-Environmental occurrence and strategies for microbial degradation. *Chemosphere*. 2021;280:130608. <https://doi.org/10.1016/j.chemosphere.2021.130608>. Epub 2021 Apr 28. PMID: 33962296.
31. Liu D, Chen S, Gou Y, et al. Gastrointestinal microbiota changes in patients with gastric precancerous lesions. *Front Cell Infect Microbiol*. 2021;11:749207. <https://doi.org/10.3389/fcimb.2021.749207>. PMID: 34956928; PMCID: PMC8695999.
32. Sung JJY, Coker OO, Chu E, et al. Gastric microbes associated with gastric inflammation, atrophy and intestinal metaplasia 1 year after *Helicobacter pylori* eradication. *Gut*. 2020;69(9):1572–80. <https://doi.org/10.1136/gutjnl-2019-319826>. Epub 2020 Jan 23. PMID: 31974133; PMCID: PMC7456733.
33. Fan HN, Zhu P, Zhang J, et al. Mucosal Microbiome dysbiosis associated with duodenum bulb inflammation. *Microb Pathog*. 2021;150:104711. <https://doi.org/10.1016/j.micpath.2020.104711>. Epub 2020 Dec 29. PMID: 33385493.
34. Tseng CH, Lin JT, Ho HJ, et al. Gastric microbiota and predicted gene functions are altered after subtotal gastrectomy in patients with gastric cancer. *Sci Rep*. 2016;6:20701. <https://doi.org/10.1038/srep20701>. PMID: 26860194; PMCID: PMC4748256.

Publisher's note

Springer Nature remains neutral with regard to jurisdictional claims in published maps and institutional affiliations.